A

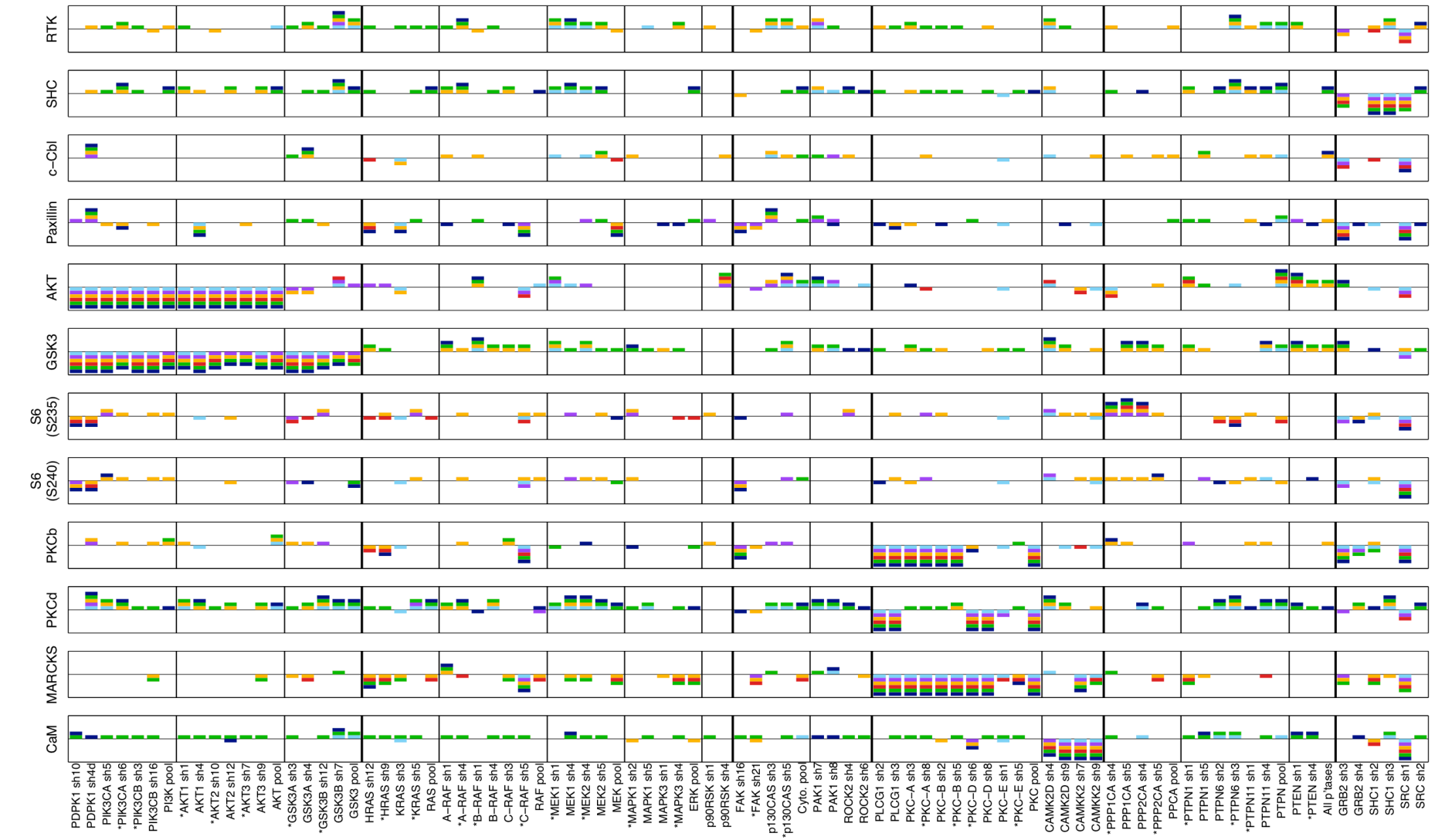
RTK
SHC
c–Cbl
Paxillin
AKT
GSK3
S6 (S235)
S6 (S240)
PKCb
PKCd
MARCKS
CaM
PDPK1 sh10
PDPK1 sh4d
PIK3CA sh5
*PIK3CA sh6
*PIK3CB sh3
PIK3CB sh16
PI3K pool
*AKT1 sh1
AKT1 sh4
*AKT2 sh10
AKT2 sh12
*AKT3 sh7
AKT3 sh9
AKT pool
*GSK3A sh3
GSK3A sh4
*GSK3B sh12
GSK3B sh7
GSK3 pool
HRAS sh12
*HRAS sh9
KRAS sh3
*KRAS sh5
RAS pool
A–RAF sh1
*A–RAF sh4
*B–RAF sh1
B–RAF sh4
C–RAF sh3
*C–RAF sh5
RAF pool
*MEK1 sh1
MEK1 sh4
*MEK2 sh4
MEK2 sh5
MEK pool
*MAPK1 sh2
MAPK1 sh5
MAPK3 sh1
*MAPK3 sh4
ERK pool
p90RSK sh1
p90RSK sh4
FAK sh16
*FAK sh21
p130CAS sh3
*p130CAS sh5
Cyto. pool
PAK1 sh7
PAK1 sh8
ROCK2 sh4
ROCK2 sh6
PLCG1 sh2
PLCG1 sh3
PKC–A sh3
*PKC–A sh8
PKC–B sh2
*PKC–B sh5
*PKC–D sh6
PKC–D sh8
PKC–E sh1
*PKC–E sh5
PKC pool
CAMK2D sh4
CAMK2D sh9
CAMKK2 sh7
CAMKK2 sh9
*PPP1CA sh4
PPP1CA sh5
PPP2CA sh4
*PPP2CA sh5
PPCA pool
*PTPN1 sh1
PTPN1 sh5
PTPN6 sh2
*PTPN6 sh3
*PTPN11 sh1
PTPN11 sh4
PTPN pool
PTEN sh1
*PTEN sh4
All p'tases
GRB2 sh3
GRB2 sh4
SHC1 sh2
SHC1 sh3
SRC sh1
SRC sh2

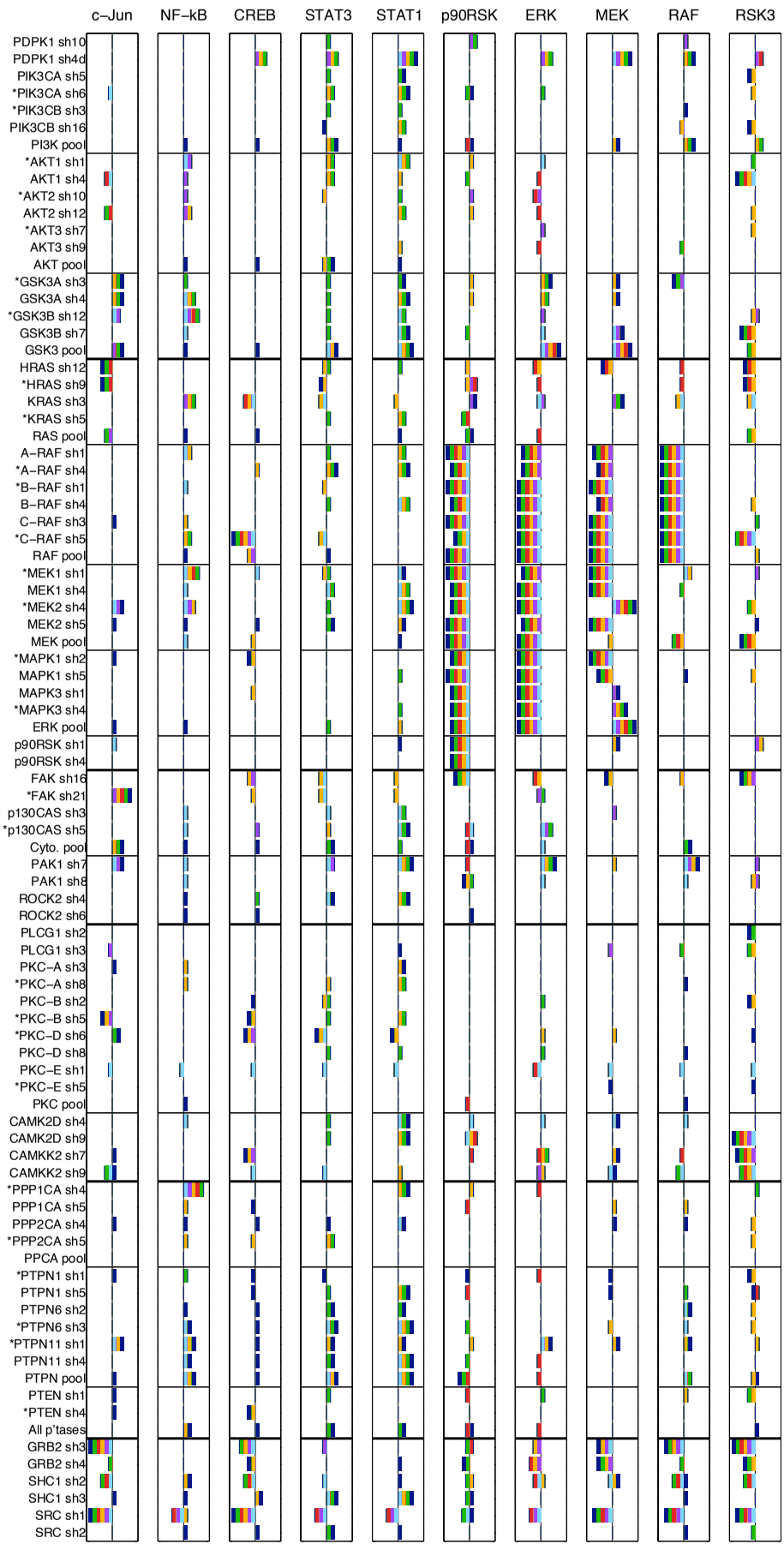
c–Jun
NF–kB
CREB
STAT3
STAT1
p90RSK
ERK
MEK
RAF
RSK3
PDPK1 sh10
PDPK1 sh4d
PIK3CA sh5
*PIK3CA sh6
*PIK3CB sh3
PIK3CB sh16
PI3K pool
*AKT1 sh1
AKT1 sh4
*AKT2 sh10
AKT2 sh12
*AKT3 sh7
AKT3 sh9
AKT pool
*GSK3A sh3
GSK3A sh4
*GSK3B sh12
GSK3B sh7
GSK3 pool
HRAS sh12
*HRAS sh9
KRAS sh3
*KRAS sh5
RAS pool
A–RAF sh1
*A–RAF sh4
*B–RAF sh1
B–RAF sh4
C–RAF sh3
*C–RAF sh5
RAF pool
*MEK1 sh1
MEK1 sh4
*MEK2 sh4
MEK2 sh5
MEK pool
*MAPK1 sh2
MAPK1 sh5
MAPK3 sh1
*MAPK3 sh4
ERK pool
p90RSK sh1
p90RSK sh4
FAK sh16
*FAK sh21
p130CAS sh3
*p130CAS sh5
Cyto. pool
PAK1 sh7
PAK1 sh8
ROCK2 sh4
ROCK2 sh6
PLCG1 sh2
PLCG1 sh3
PKC–A sh3
*PKC–A sh8
PKC–B sh2
*PKC–B sh5
*PKC–D sh6
PKC–D sh8
PKC–E sh1
*PKC–E sh5
PKC pool
CAMK2D sh4
CAMK2D sh9
CAMKK2 sh7
CAMKK2 sh9
*PPP1CA sh4
PPP1CA sh5
PPP2CA sh4
*PPP2CA sh5
PPCA pool
*PTPN1 sh1
PTPN1 sh5
PTPN6 sh2
*PTPN6 sh3
*PTPN11 sh1
PTPN11 sh4
PTPN pool
PTEN sh1
*PTEN sh4
All p'tases
GRB2 sh3
GRB2 sh4
SHC1 sh2
SHC1 sh3
SRC sh1
SRC sh2

B

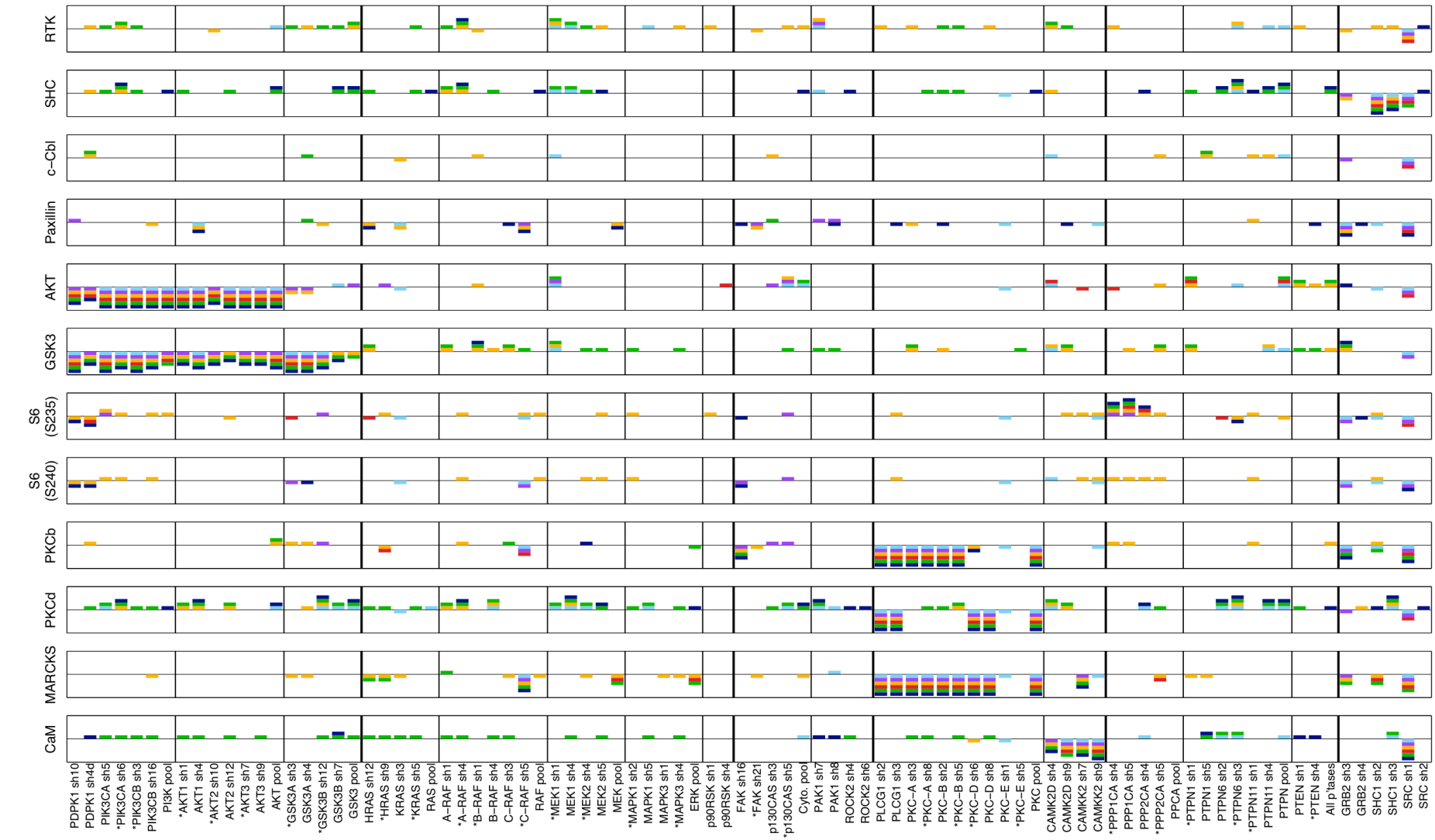
RTK
SHC
c–Cbl
Paxillin
AKT
GSK3
S6 (S235)
S6 (S240)
PKCb
PKCd
MARCKS
CaM
PDPK1 sh10
PDPK1 sh4d
PIK3CA sh5
*PIK3CA sh6
*PIK3CB sh3
PIK3CB sh16
PI3K pool
*AKT1 sh1
AKT1 sh4
*AKT2 sh10
AKT2 sh12
*AKT3 sh7
AKT3 sh9
AKT pool
*GSK3A sh3
GSK3A sh4
*GSK3B sh12
GSK3B sh7
GSK3 pool
HRAS sh12
*HRAS sh9
KRAS sh3
*KRAS sh5
RAS pool
A–RAF sh1
*A–RAF sh4
*B–RAF sh1
B–RAF sh4
C–RAF sh3
*C–RAF sh5
RAF pool
*MEK1 sh1
MEK1 sh4
*MEK2 sh4
MEK2 sh5
MEK pool
*MAPK1 sh2
MAPK1 sh5
MAPK3 sh1
*MAPK3 sh4
ERK pool
p90RSK sh1
p90RSK sh4
FAK sh16
*FAK sh21
p130CAS sh3
*p130CAS sh5
Cyto. pool
PAK1 sh7
PAK1 sh8
ROCK2 sh4
ROCK2 sh6
PLCG1 sh2
PLCG1 sh3
PKC–A sh3
*PKC–A sh8
PKC–B sh2
*PKC–B sh5
*PKC–D sh6
PKC–D sh8
PKC–E sh1
*PKC–E sh5
PKC pool
CAMK2D sh4
CAMK2D sh9
CAMKK2 sh7
CAMKK2 sh9
*PPP1CA sh4
PPP1CA sh5
PPP2CA sh4
*PPP2CA sh5
PPCA pool
*PTPN1 sh1
PTPN1 sh5
PTPN6 sh2
*PTPN6 sh3
*PTPN11 sh1
PTPN11 sh4
PTPN pool
PTEN sh1
*PTEN sh4
All p'tases
GRB2 sh3
GRB2 sh4
SHC1 sh2
SHC1 sh3
SRC sh1
SRC sh2

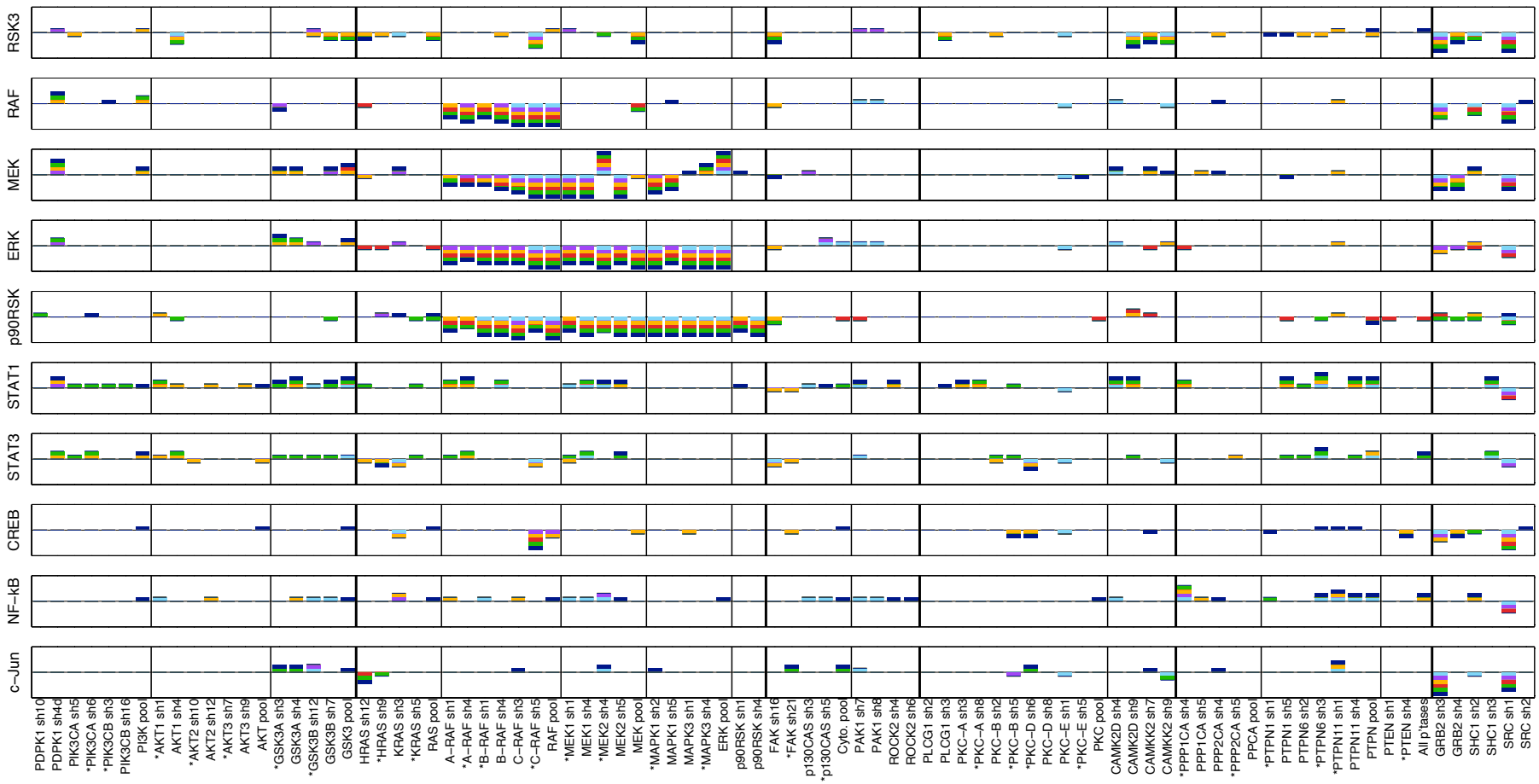

Figure S1. shRNA effects for individual shRNAs. (A) 1% Storey FDR correction (less conservative). (B) 1% Benjamini FDR correction (more conservative). The representation chosen here contrasts with Fig. 2, in which the heatmap only indicates cases where both shRNAs gave significant and consistent effects. Stacked bars indicate binary increase/decrease effects. For a given phosphosite row, stacked bars above or below the horizontal line indicate increased or decreased signal effects, respectively. The six colors represent the six RTKs by the same color scheme as used in the main text, as initially introduced in Fig. 1: cyan, EGFR; purple, FGFR1; yellow, IGF-1R; red, c-Met; green, NTRK2; blue, PDGFRβ. Asterisks indicate shRNAs used in pools. Phosphosite rows and shRNA columns are organized by approximate pathway membership. Thin vertical lines separate different shRNA pools. Thick vertical lines separate shRNAs by approximate pathways.

RTK
SHC
c−Cbl
Paxillin
AKT
GSK3
S6 (S235)
S6 (S240)
PKCb
PKCd
MARCKS
CaM
2
1
0
−1
−2
PDPK1 sh10
PDPK1 sh4d
PIK3CA sh5
*PIK3CA sh6
*PIK3CB sh3
PIK3CB sh16
PI3K pool
*AKT1 sh1
AKT1 sh4
*AKT2 sh10
AKT2 sh12
*AKT3 sh7
AKT3 sh9
AKT pool
*GSK3A sh3
GSK3A sh4
*GSK3B sh12
GSK3B sh7
GSK3 pool
HRAS sh12
*HRAS sh9
KRAS sh3
*KRAS sh5
RAS pool
A−RAF sh1
*A−RAF sh4
*B−RAF sh1
B−RAF sh4
C−RAF sh3
*C−RAF sh5
RAF pool
*MEK1 sh1
MEK1 sh4
*MEK2 sh4
MEK2 sh5
MEK pool
*MAPK1 sh2
MAPK1 sh5
MAPK3 sh1
*MAPK3 sh4
ERK pool
p90RSK sh1
p90RSK sh4
FAK sh16
*FAK sh21
p130CAS sh3
*p130CAS sh5
Cyto. pool
PAK1 sh7
PAK1 sh8
ROCK2 sh4
ROCK2 sh6
PLCG1 sh2
PLCG1 sh3
PKC−A sh3
*PKC−A sh8
PKC−B sh2
*PKC−B sh5
*PKC−D sh6
PKC−D sh8
PKC−E sh1
*PKC−E sh5
PKC pool
CAMK2D sh4
CAMK2D sh9
CAMKK2 sh7
CAMKK2 sh9
*PPP1CA sh4
PPP1CA sh5
PPP2CA sh4
*PPP2CA sh5
PPCA pool
*PTPN1 sh1
PTPN1 sh5
PTPN6 sh2
*PTPN6 sh3
*PTPN11 sh1
PTPN11 sh4
PTPN pool
PTEN sh1
*PTEN sh4
All p'tases
GRB2 sh3
GRB2 sh4
SHC1 sh2
SHC1 sh3
SRC sh1
SRC sh2

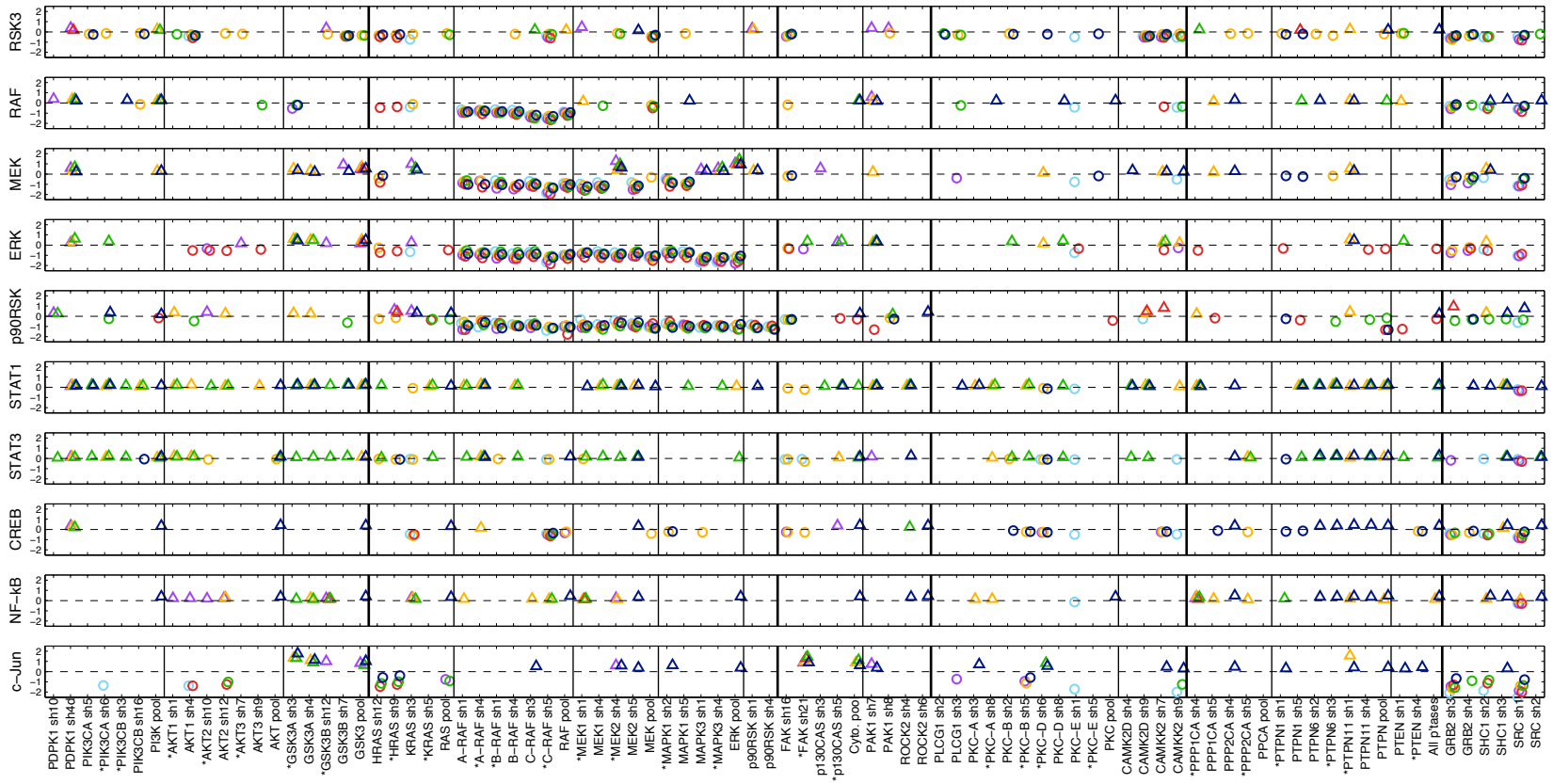

Figure S2. Quantitative shRNA-induced effects for individual shRNAs. In contrast to the binary increase/decrease effects shown in Fig. S1, here the real-valued shRNA effects are shown (using the 1% Storey FDR, as in Fig. S1A). The y-axis of each phosphosite row now represents the $\log_2$ value of (median AUC of test shRNA across four biological replicates / median AUC of control shRNA). The median control shRNA AUC was calculated as the median AUC value across the three control shRNAs' four biological replicates (i.e., a median of 12 AUC values). Triangle and circle markers represent increased and decreased signal effects, respectively. The six colors represent the six RTKs by the same color scheme as used in the main text, as initially introduced in Fig. 1: cyan, EGFR; purple, FGFR1; yellow, IGF-1R; red, c-Met; green, NTRK2; blue, PDGFRβ. Asterisks indicate shRNAs used in pools. Phosphosite rows and shRNA columns are organized by approximate pathway membership. Thin vertical lines separate different shRNA pools. Thick vertical lines separate shRNAs by approximate pathways of their target genes.

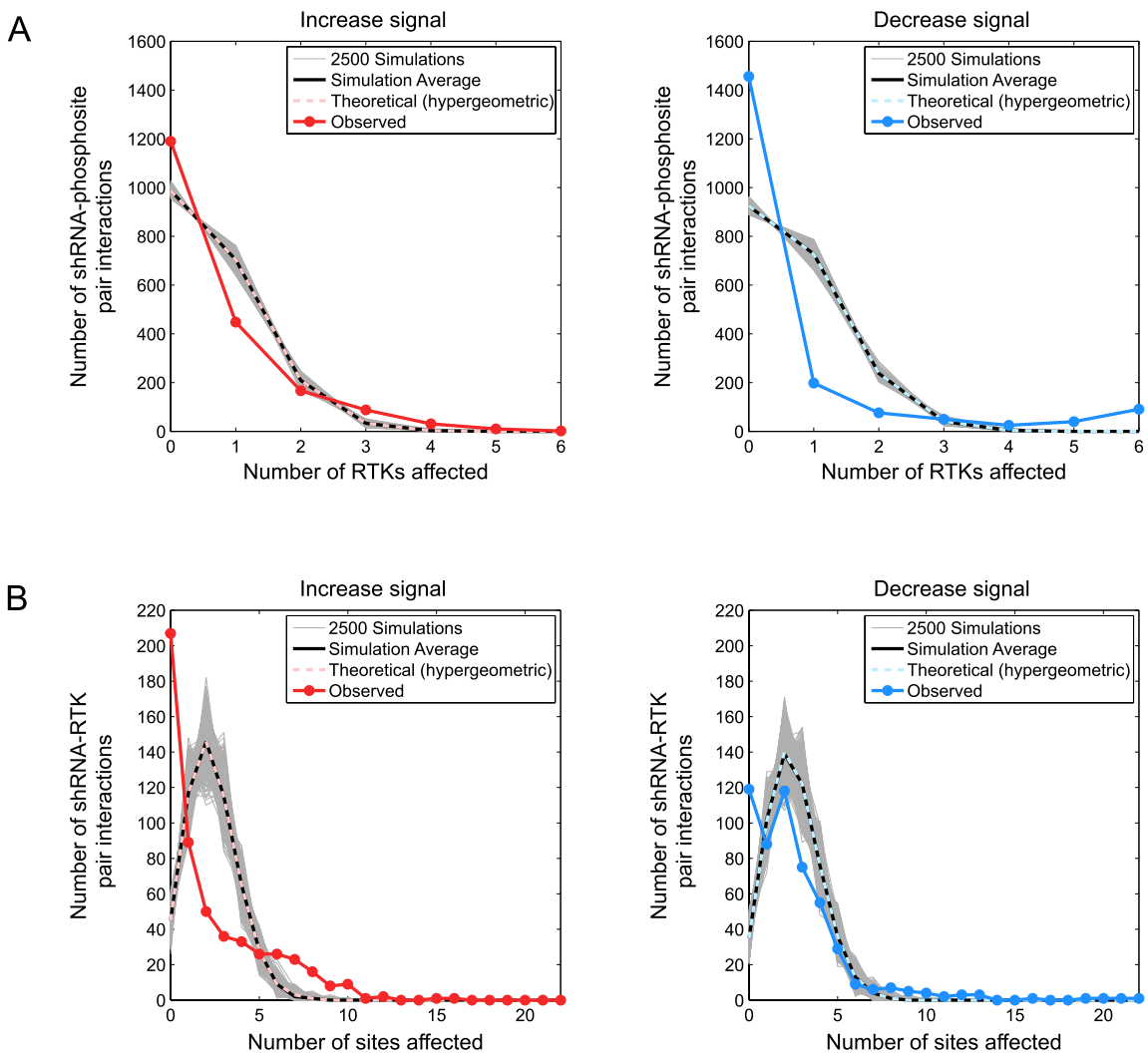

Figure S3. Observed shRNA-induced effects across (A) RTKs and (B) phosphosites are not consistent with a model in which shRNA effects are randomly distributed. The total number of increased (1,232) and decreased (1,346) signal effects resulting from the Storey 1% FDR correction were randomly distributed *in silico* among the 11,616 RTK-shRNA-phosphosite pairs (6 RTKs x 88 shRNAs x 22 phosphosites). The number of increased and decreased signal effects was then tallied across the RTKs and across the phosphosites. This simulation was repeated 2,500 times. The simulation average converged to the hypergeometric distribution. Because the distributions of randomly distributed shRNA effects are not consistent with the distributions of observed shRNA effects, often with empirical p << 4e-4 (1/2,500) when comparing individual values in the distributions, we conclude that the distributions of shRNA effects across RTKs and across phosphosites are significantly non-random.

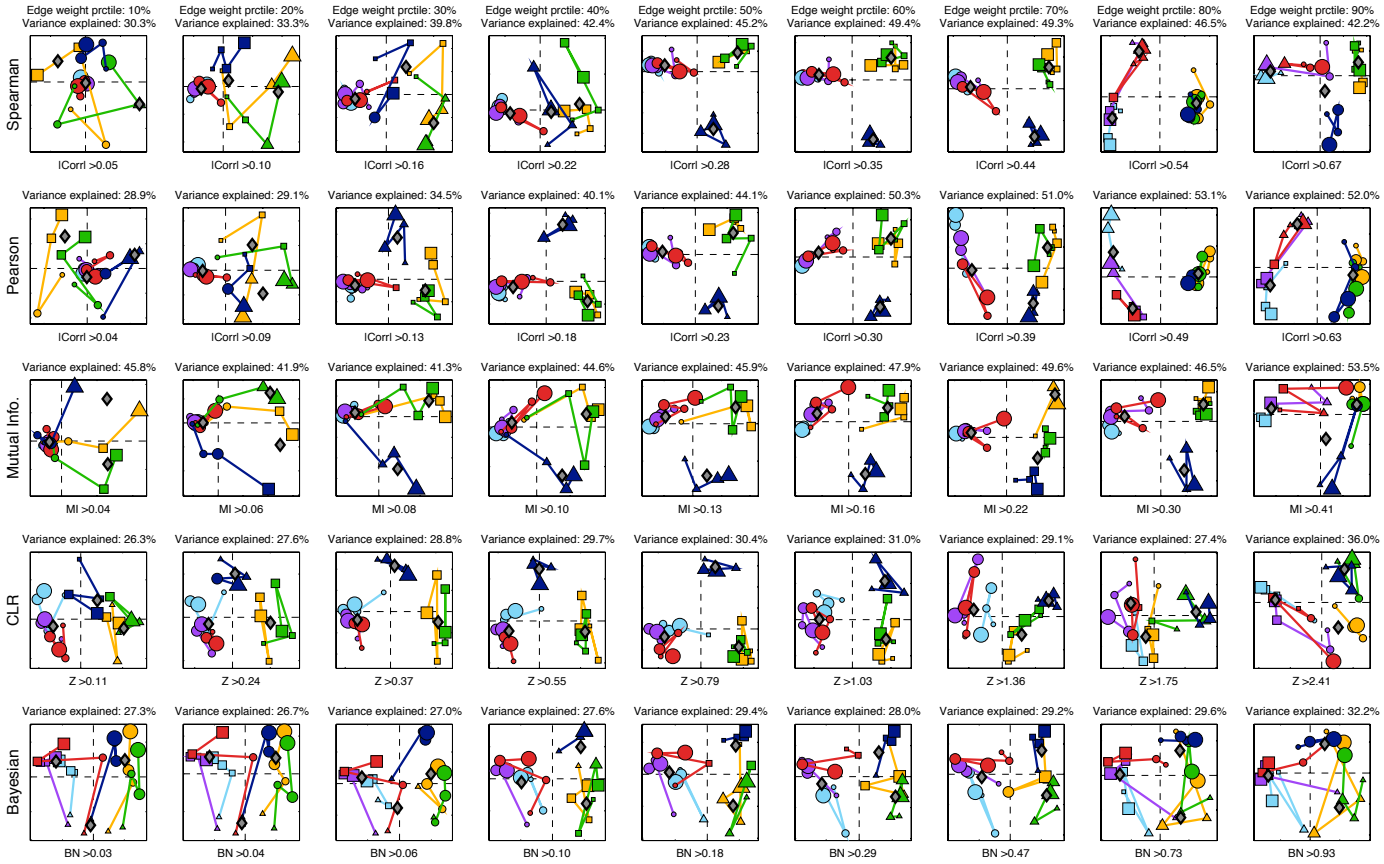

Figure S4. Network model clusters are robust to applied edge weight threshold. Results for clustering the network model structures, here visualized using the first two eigenvalues from multidimensional scaling, for each of the five inference methods across a range of edge weight thresholds. Thresholds were determined by varying the percentile ranking of edge weights for each method. Percentiles increase from left to right, and are indicated at the top of each row. Plot marker shapes indicate cluster assignments, while marker size indicates time scale (basal = smallest, late = largest). The six colors represent the six RTKs by the same color scheme as used in the main text, as initially introduced in Fig. 1: cyan, EGFR; purple, FGFR1; yellow, IGF-1R; red, c-Met; green, NTRK2; blue, PDGFRβ.

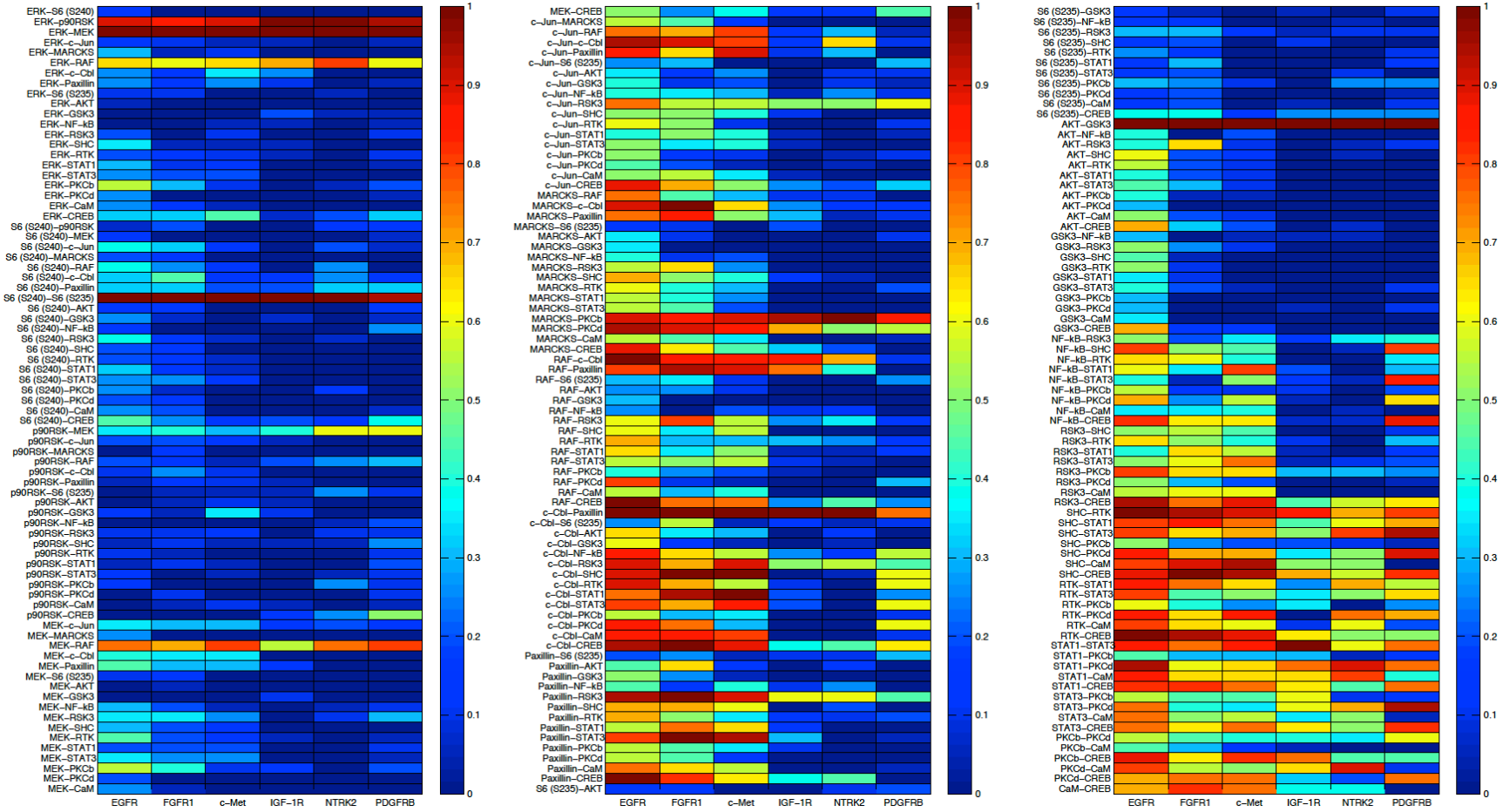

Figure S5. Identifying RTK class-specific edges through consensus network edge frequency. Heatmap values indicate the fraction of network models (when considering all five inference methods and all four time scales) containing the indicated edge.

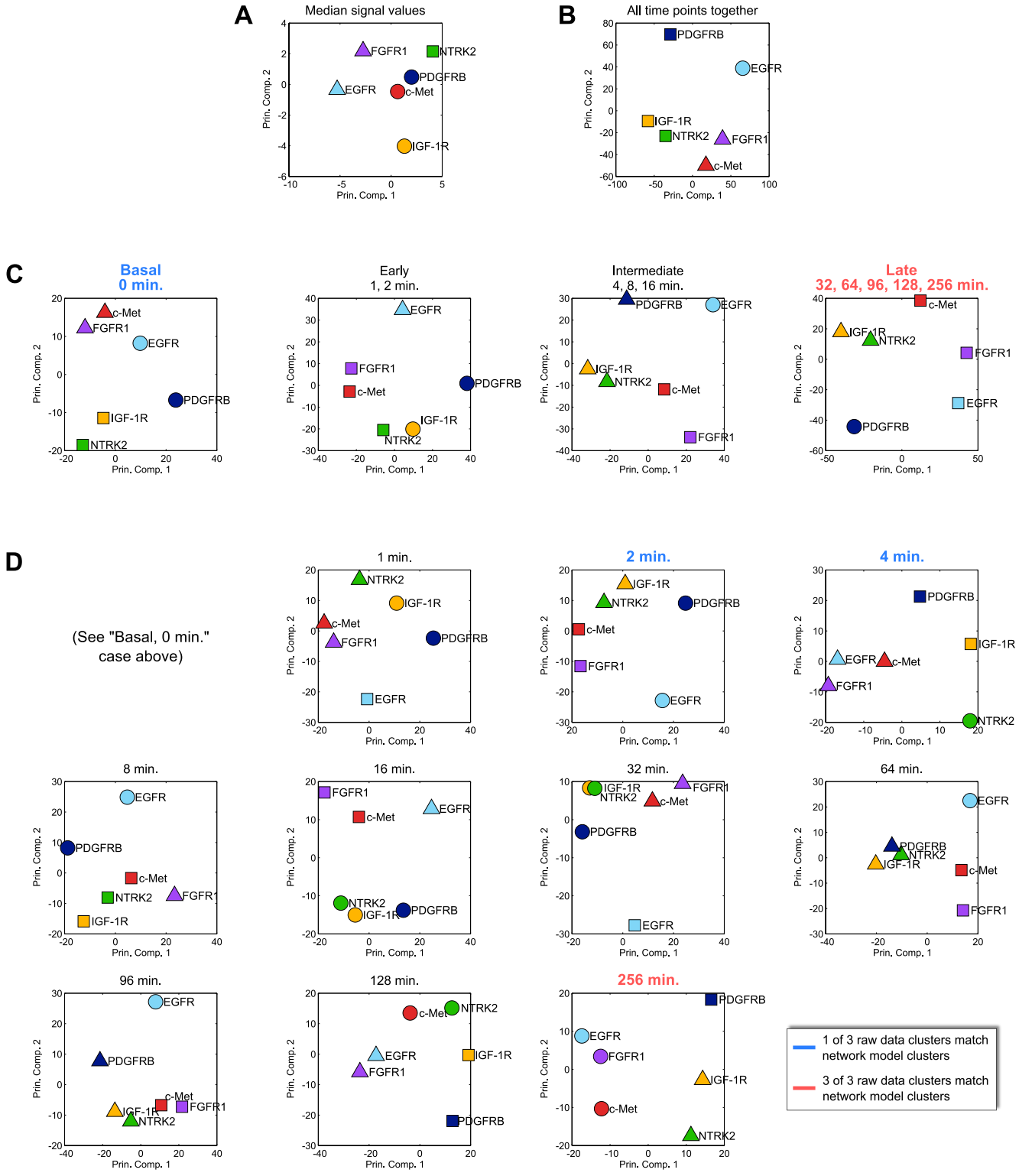

Figure S6. Clustering the raw data directly. The raw data were clustered using (A) the median signal values, (B) all time points together, (C) each time scale separately, or (D) individual time points. Cases where one of three raw data clusters matched the network model clusters are shown with blue titles, while cases where all three raw data clusters matched the network model clusters are shown with red titles. Marker shapes indicate cluster assignments. The six marker colors represent the six RTKs by the same color scheme as used in the main text, as initially introduced in Fig. 1: cyan, EGFR; purple, FGFR1; yellow, IGF-1R; red, c-Met; green, NTRK2; blue, PDGFRβ.

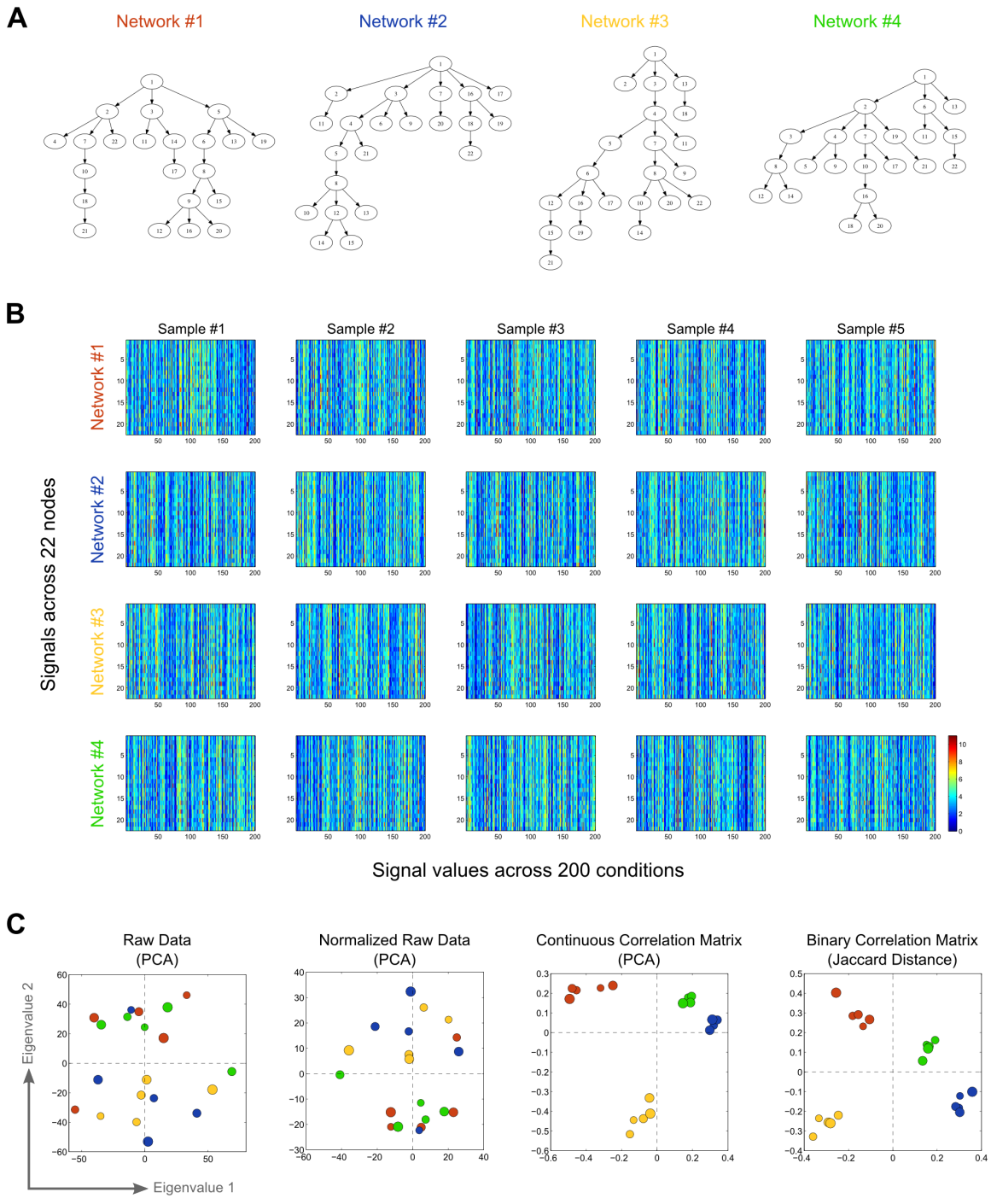

Figure S7. Clustering inferred network topologies reveals underlying network differences but clustering raw data does not. (A) Four synthetic networks used to simulate data. Network structures are defined based on edges between individually numbered nodes, whose positions vary from network to network. (B) Simulated data sets for five independent samples from each of the four networks. Rows of each heatmap represent nodes and columns represent conditions. All heatmaps are shown using the same colorbar scale. (C) Using principal component analysis to visualize the raw data, normalized raw data, and Spearman correlation matrices, and multidimensional scaling to visualize the binary Spearman correlation matrix (correlation values exceeding the 60th percentile). Marker colors indicate which of the four synthetic networks the data were generated from. The inferred network topologies (i.e., correlation matrices) cluster according to their underlying networks, but the raw data do not.

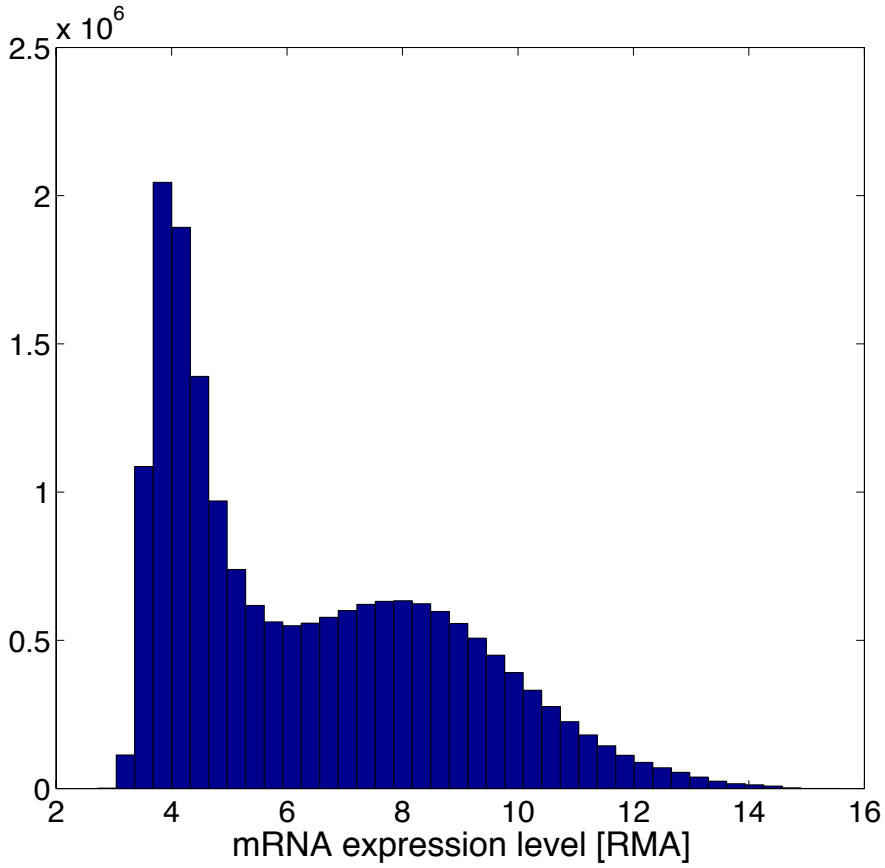

Figure S8. Observed distribution of gene expression values in the CCLE. All gene expression values in the CCLE were included (when considering all 18,926 genes across all 967 cell lines, i.e., 18,926 x 967 ~ 18.3 million gene expression values). The bimodal nature of the plot suggested a natural range over which to consider genes to be expressed versus not expressed.

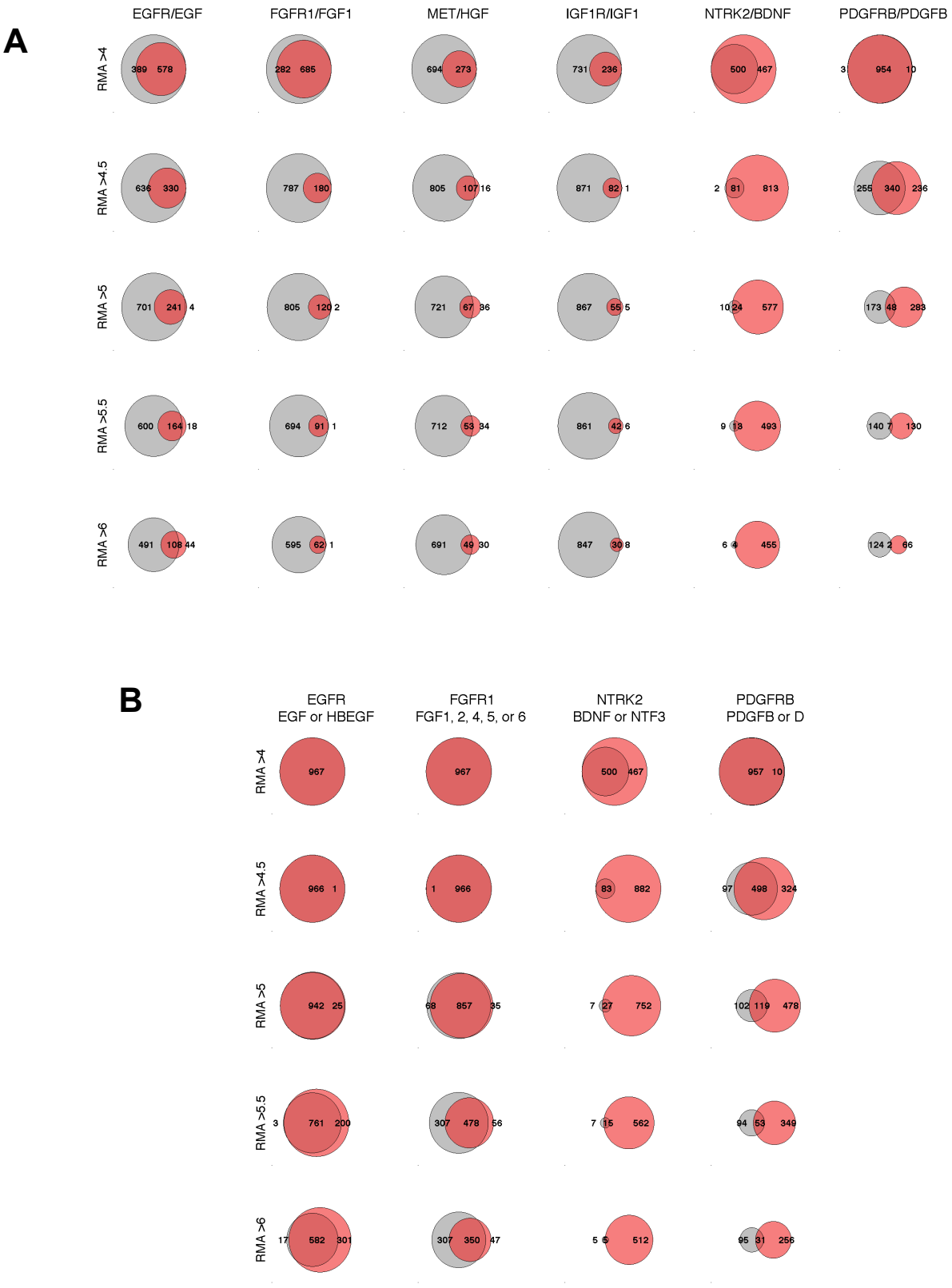

Figure S9. Co-expression of the receptors and ligands for multiple RMA thresholds. The co-expression of receptors and cognate ligands, as shown by Venn diagrams, are robust to the RMA threshold used to define expression when considering (A) only ligands used in this study, or (B) multiple RTK-activating ligands. Different RMA thresholds are shown down the rows, while different RTKs are shown across columns.

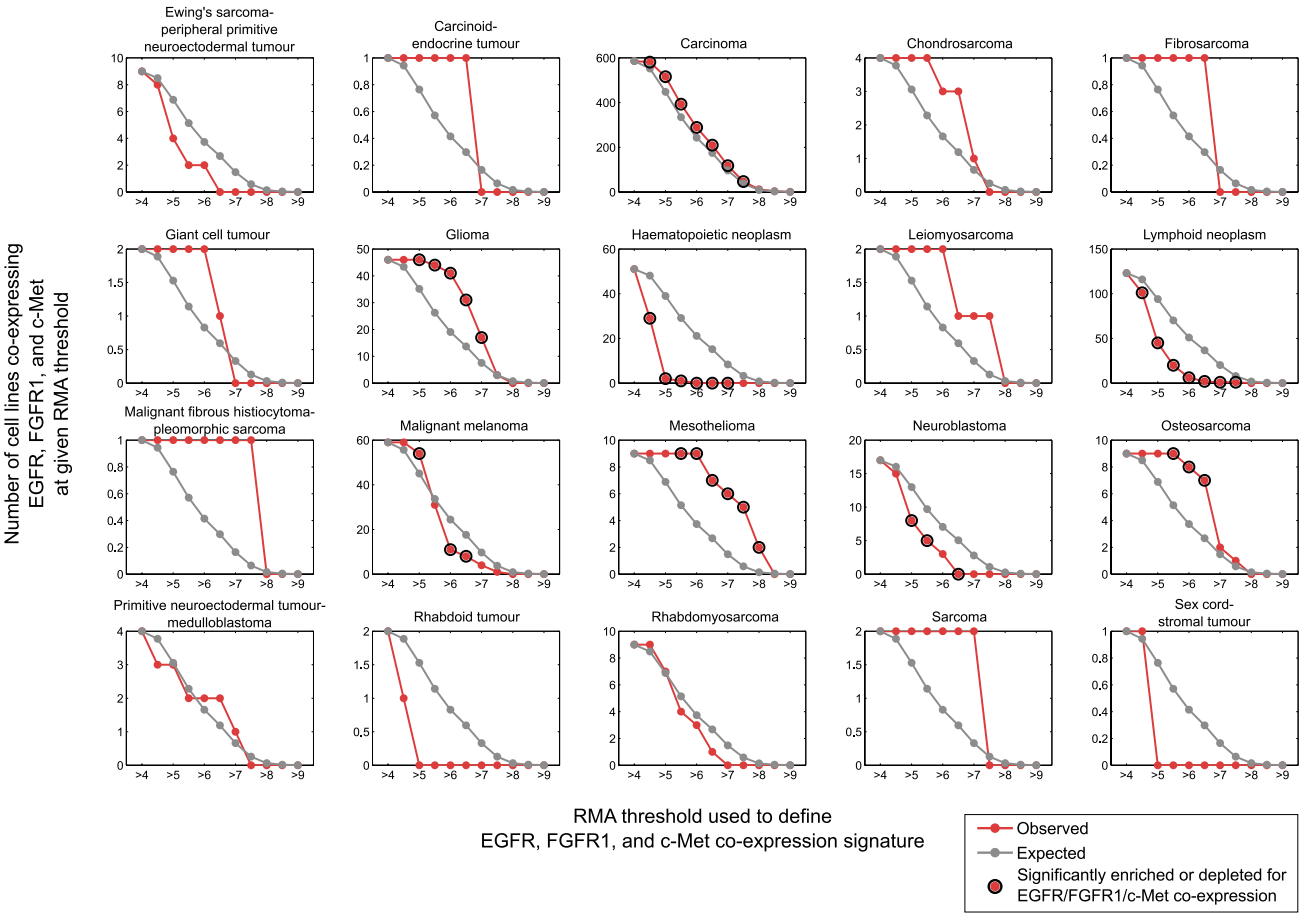

Figure S10. Cell line histology enrichment results for multiple RMA thresholds. The enrichment or depletion of cell lines with *EGFR*/*FGFR1*/*MET* co-expression in cell lines with different histological origins are shown. The values on the x-axis indicate the RMA threshold used to first identify which cell lines were co-expressing the three RTKs. Using the hypergeometric distribution, grey data points indicate the expected number of cell lines from each histology type that should also co-express these three RTKs. Red data points indicate the actual observed number of cell lines from each histology type that also co-express these three RTKs. Note that subplots have different y-axis scales. Significance (indicated by black circles) was determined using a 5% FDR ($p < 0.0191$) with the Benjamini method.

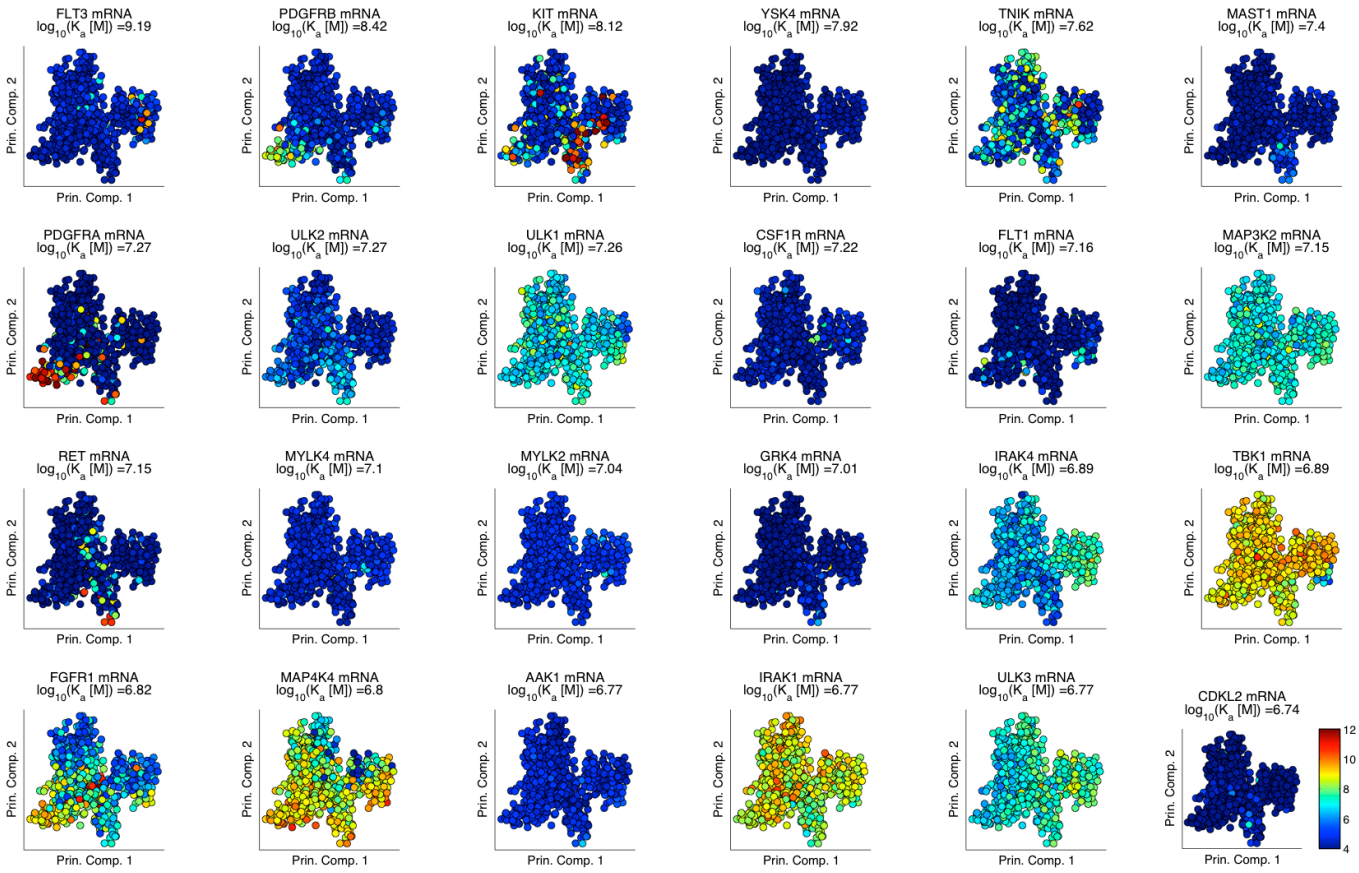

Figure S11. Gene expression values of tightest TKI258 kinase binders. The gene expression values of the 24 kinases that bind TKI258 most tightly are shown, as indicated by the color of each marker in principal component space (analogous to the plots in Fig. 5C). Kinases are sorted in order of decreasing affinity from upper left to lower right. Each marker corresponds to one cell line in the CCLE. Although TKI258 binds to 18 kinases more tightly than it binds to FGFR1, many of these other binders are expressed at low levels in the CCLE. All subplots are shown on the same color scale.

A

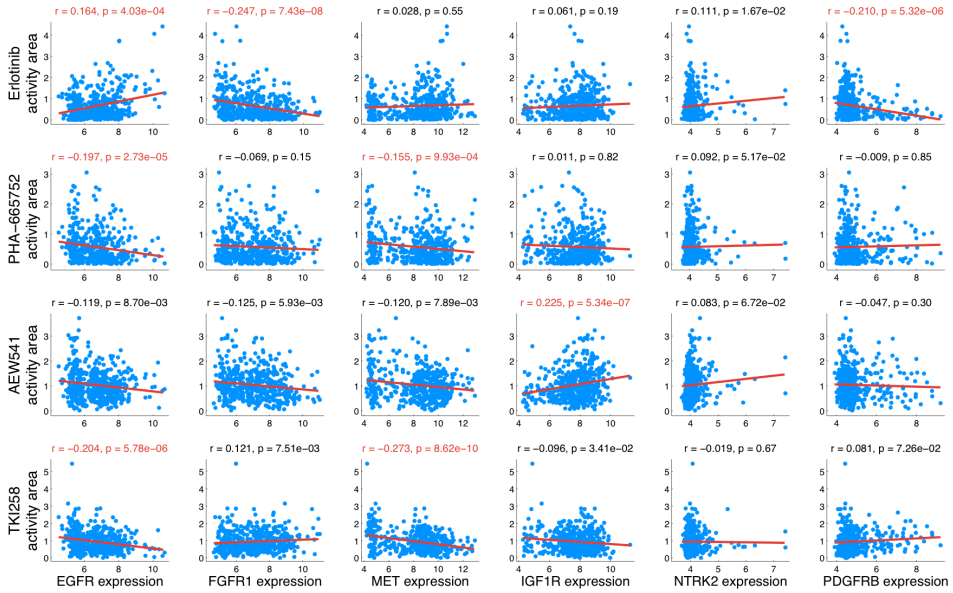

B

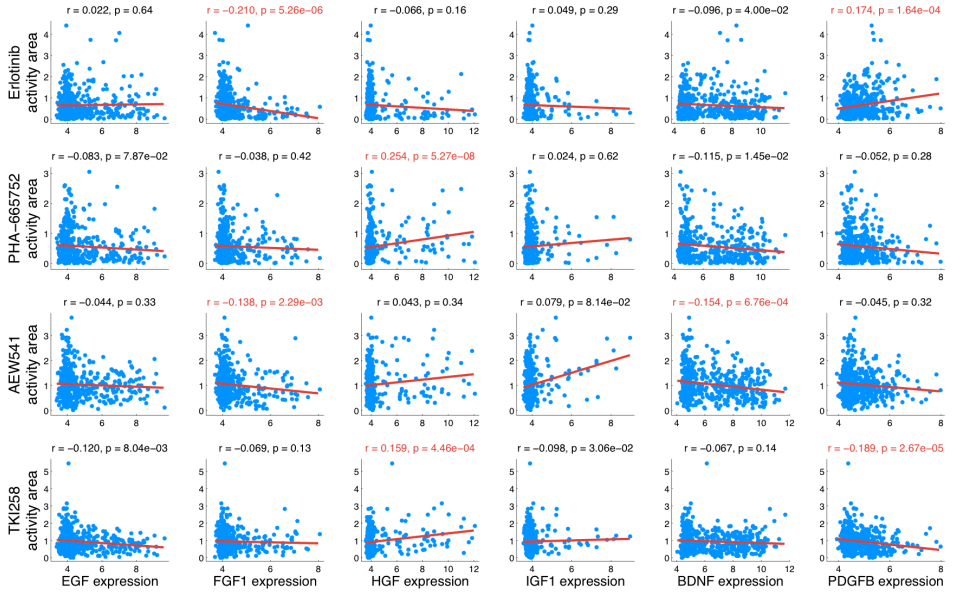

Figure S12. Correlating RTK and ligand gene expression with drug response. Plots showing gene expression values versus drug activity area are shown for the six RTKs and six ligands versus four different drugs. These plots and Spearman correlation values are repeated at different RMA thresholds used to define expression. Cell lines used in the correlation calculation are shown in blue. The red line in each plot indicates the linear fit to the data and is intended to give a visual representation of the trends in the data. Significant Spearman correlation coefficients (1% Benjamini FDR) have red subplot titles. Only considering cell lines expressing (A) receptor and (B) ligand genes with an RMA threshold >0.

C

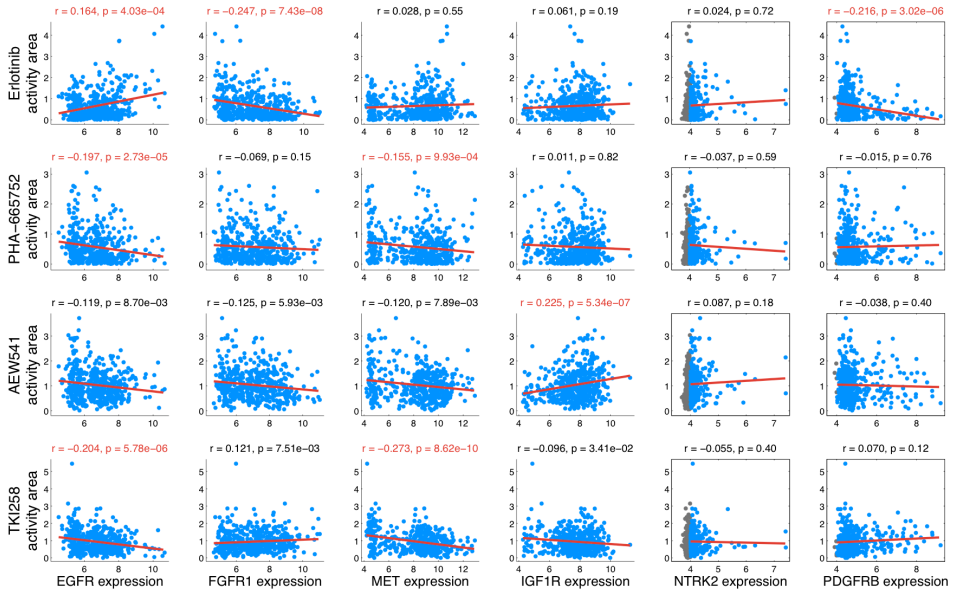

D

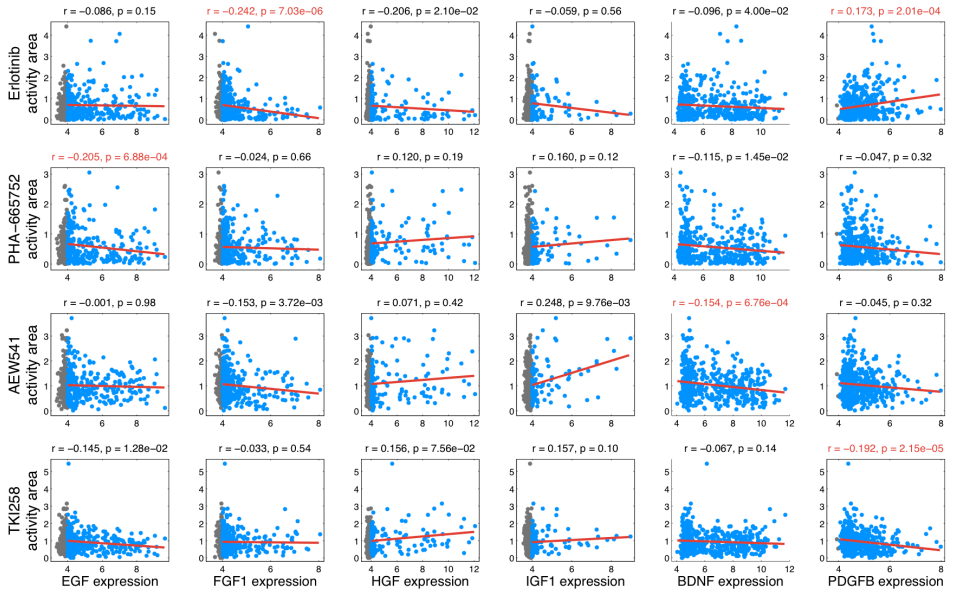

Figure S12 (continued). Only considering cell lines expressing (C) receptor and (D) ligand genes with an RMA threshold >4.

E

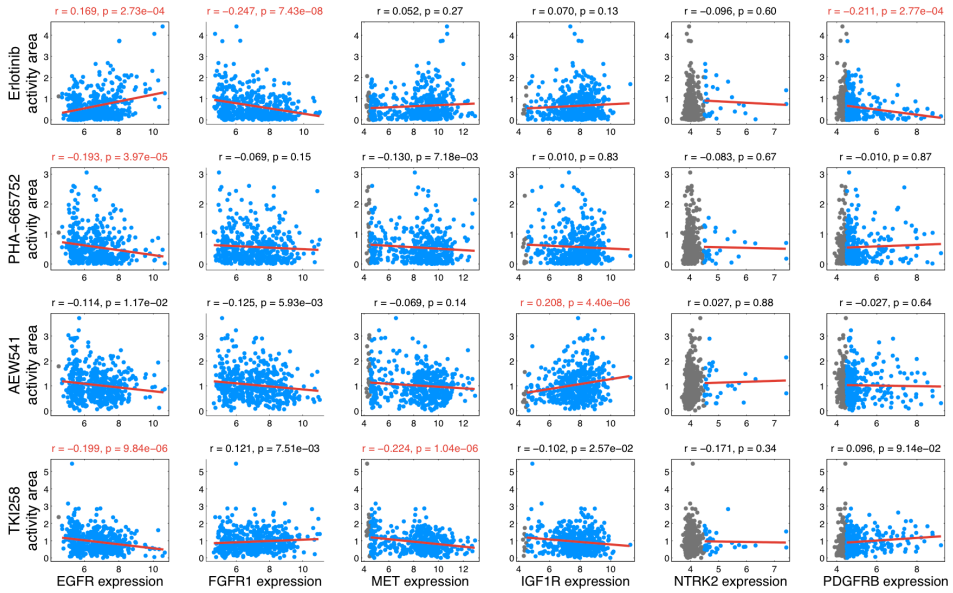

F

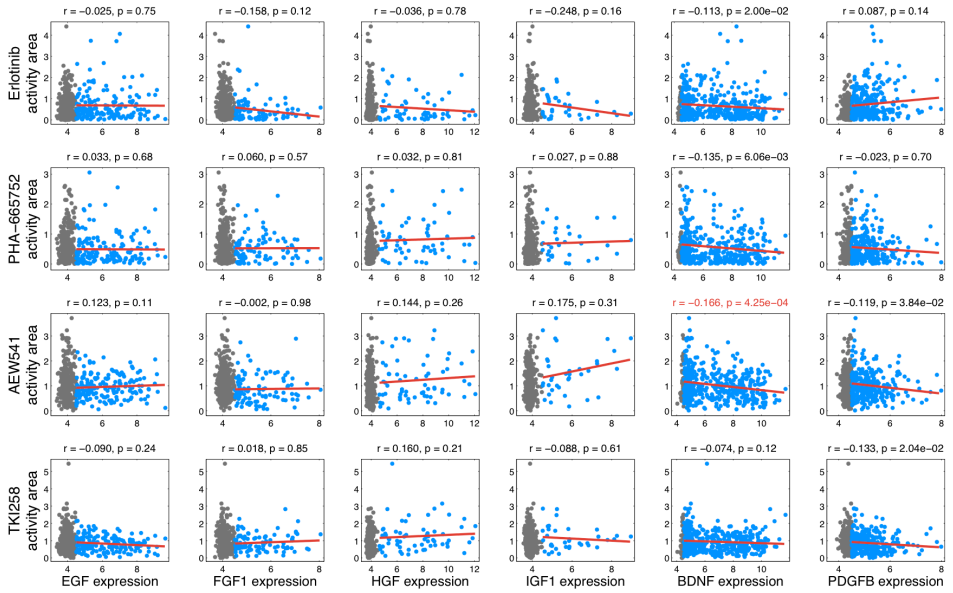

Figure S12 (continued). Only considering cell lines expressing (E) receptor and (F) ligand genes with an RMA threshold >4.5.

G

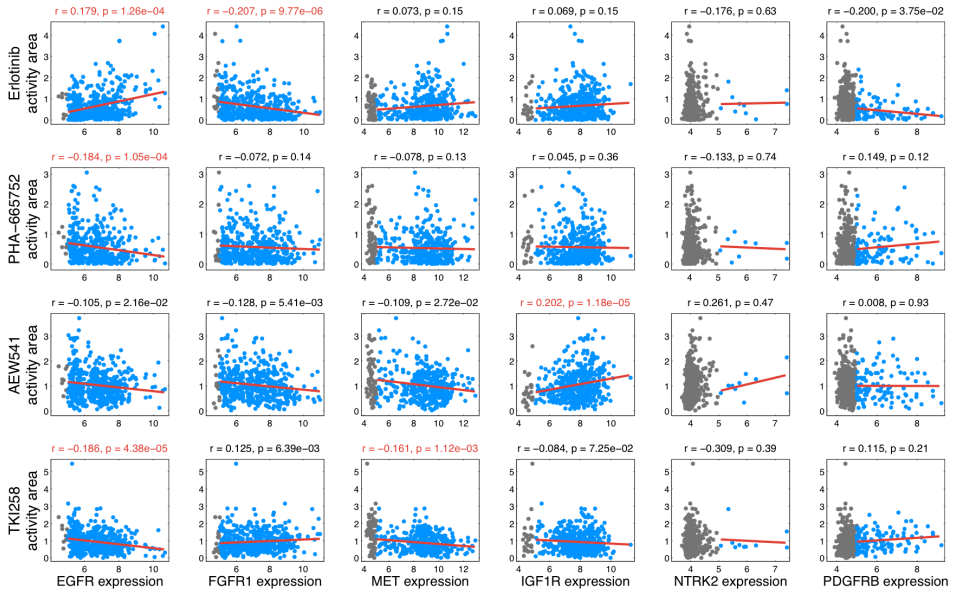

H

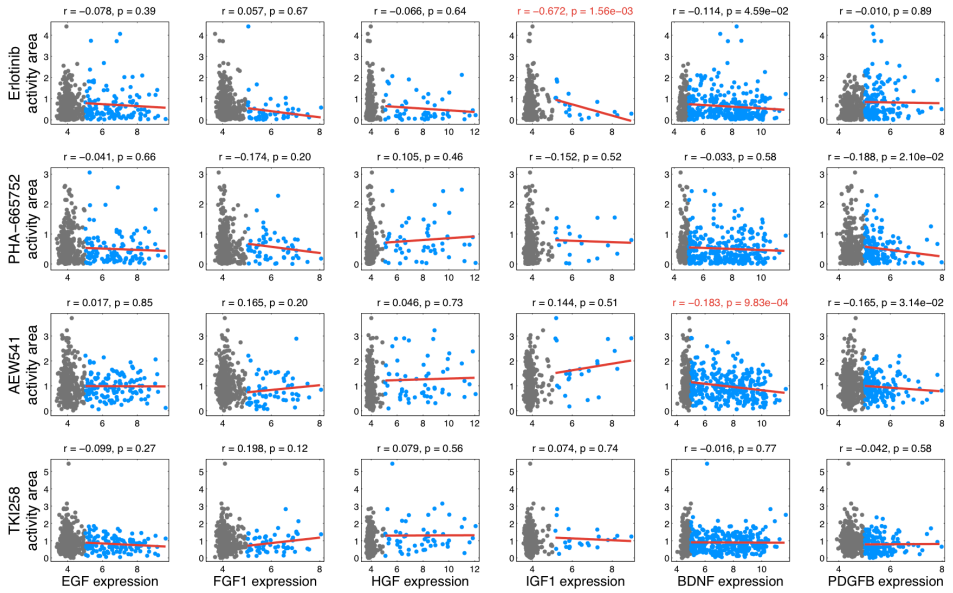

Figure S12 (continued). Only considering cell lines expressing (G) receptor and (H) ligand genes with an RMA threshold >5.

I

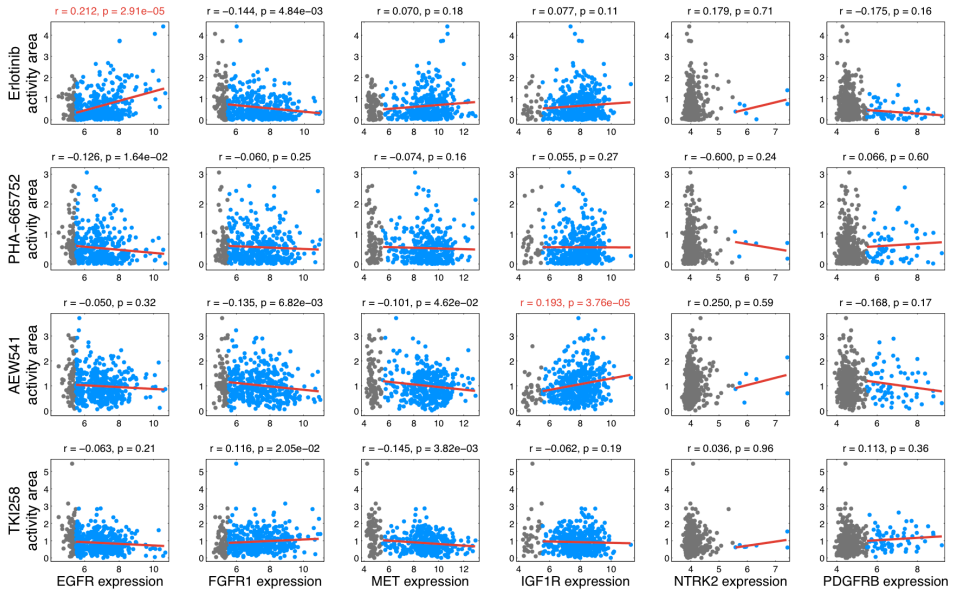

J

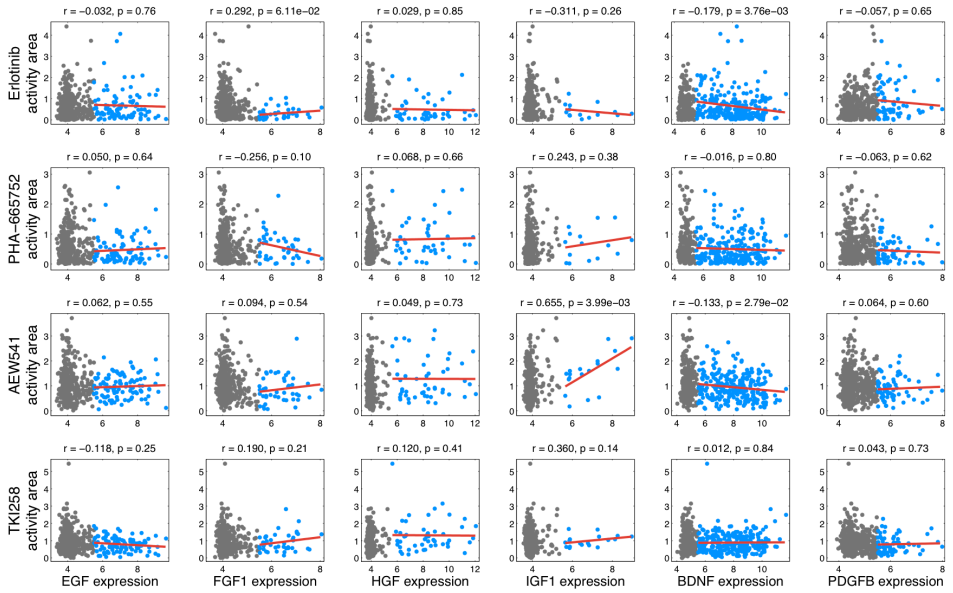

Figure S12 (continued). Only considering cell lines expressing (I) receptor and (J) ligand genes with an RMA threshold >5.5.

K

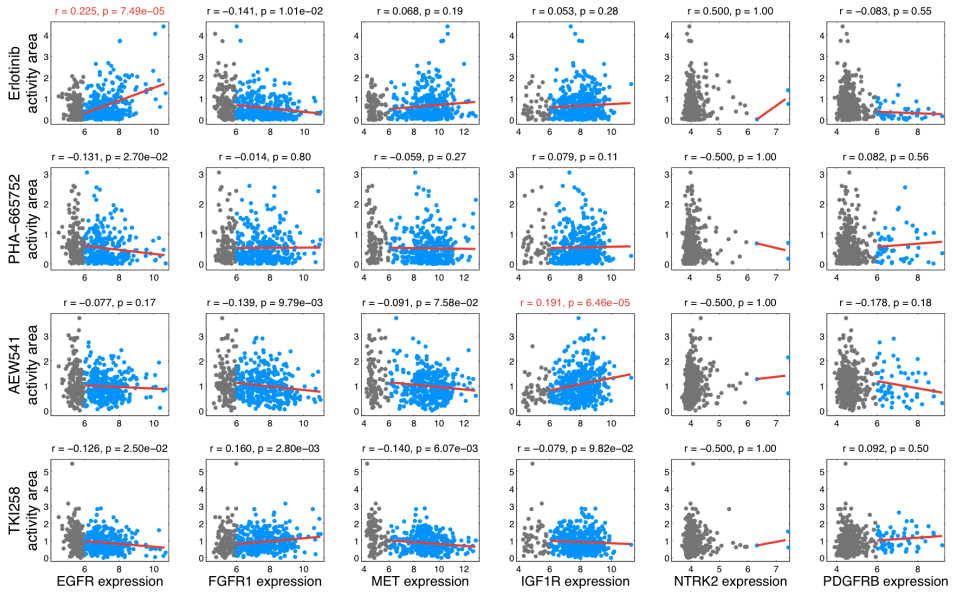

L

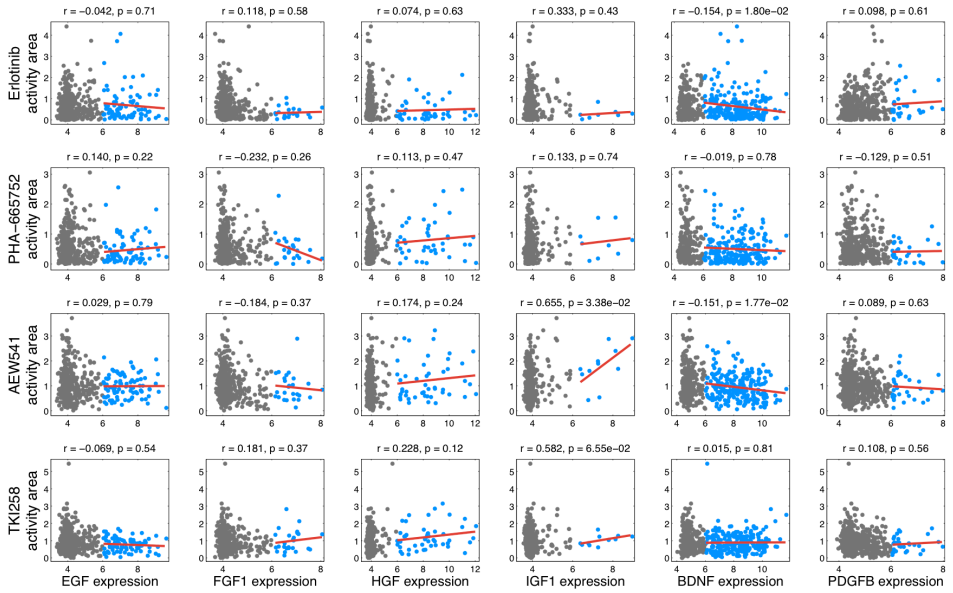

Figure S12 (continued). Only considering cell lines expressing (K) receptor and (L) ligand genes with an RMA threshold >6.

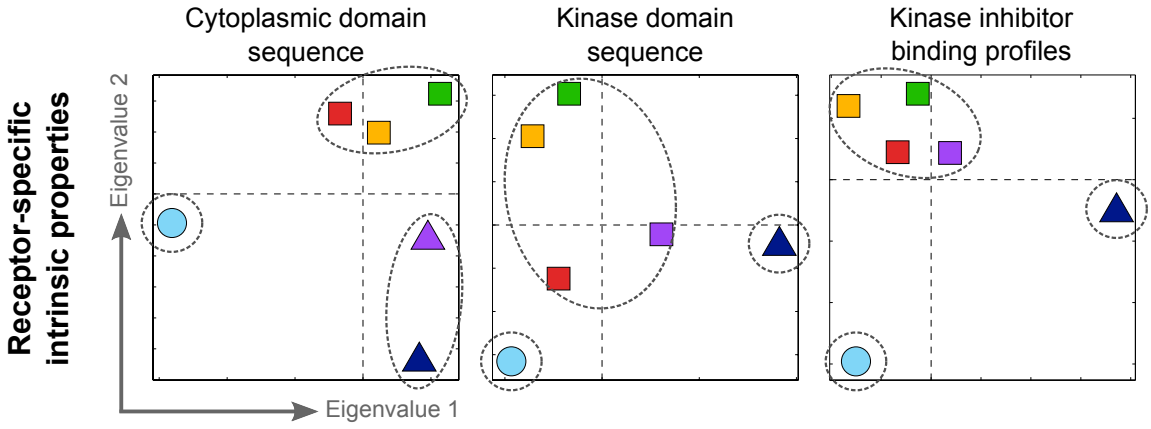

Figure S13. Clustering RTK biophysical properties does not reveal RTK network model clusters. The cytoplasmic sequences and kinase domain sequences were each clustered across the six RTKs, but did not reveal the same clusters as the RTK network models. Data concerning the affinity of each RTK for numerous small molecule kinase inhibitors was also clustered, but again did not match the network model clusters. Dotted ellipses and marker shapes represent k-means clustering assignments. The six marker colors represent the six RTKs by the same color scheme as used in the main text, as initially introduced in Fig. 1: cyan, EGFR; purple, FGFR1; yellow, IGF-1R; red, c-Met; green, NTRK2; blue, PDGFRβ.